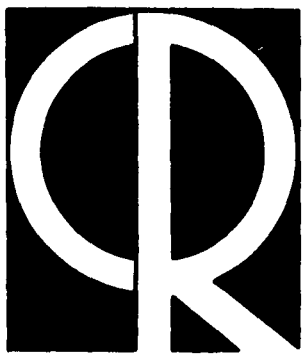

Research Translation

T-R-396+

# Determination of the Excitation Functions of the Energy Levels of Hg Atoms According to Optical Excitation Functions

I. P. ZAPESOCHNYI

RESEARCH LIBRARY

AIR FORCE CAMBRIDGE RESEARCH LABORATORIES, OFFICE OF AEROSPACE RESEARCH, UNITED STATES AIR FORCE, L. G. HANSCOM FIELD, MASS.

AMERICAN METEOROLOGICAL SOCIETY
45 BEACON STREET
BOSTON 8, MASSACHUSETTS

TRANSLATION OF

# DETERMINATION OF THE EXCITATION FUNCTIONS OF THE ENERGY LEVELS OF Hg ATOMS ACCORDING TO OPTICAL EXCITATION FUNCTIONS

( Opredelenie funktsii vozbuzhdeniia energeticheskikh urovnei atomov rtuti no opticheskim funktsiiam vozbuzhdeniia)

by

I. P. Zapesochnyi

Leningradskii Universitet Vestnik, No. 11: 67-93, 1954.

This translation has been made by the American Meteorological Society under Contract AF 19(604)-6113, through the support and sponsorship of the

AIR FORCE CAMBRIDGE RESEARCH LABORATORIES

L. G. HANSCOM FIELD

BEDFORD, MASSACHUSETTS

T-R-396+

1. Determination of the excitation functions of the energy levels of Hg atoms according to optical excitation functions

2. Opredelenie funktsii vozbuzhdeniia energeticheskikh urovnei atomov rtuti no opticheskim funktsiiam vozbuzhdeniia

3. Zapesochnyi, I. P. Leningradskii Universitet Vestnik, No. 11: 67-93, 1954.

4. 40 Typewritten pages

5. Date of translation: June 1962

6. Translator: Myron Ricci - Edited by R. M. Holden

7. Translated for Air Force Cambridge Research Laboratories, Office of Aerospace Research, United States Air Force, L. G. Hanscom Field, Bedford, Massachusetts, by the American Meteorological Society, Contract Number AF 19(604)-6113.

8. Unclassified

9. Complete

# DETERMINATION OF THE EXCITATION FUNCTIONS OF THE ENERGY LEVELS OF Hg ATOMS ACCORDING TO OPTICAL EXCITATION FUNCTIONS

by

I. P. Zapesochnyi

## 1. Excitation Functions and an Analysis of the Conditions of their Experimental Determination

Optical excitation functions which give the relationship between the intensity of spectral lines and the energy of exciting electrons, were experimentally studied by many authors. The first works on the determination of the excitation functions of spectral lines were made with rather primitive devices. A substantial success in the study of optical excitation functions was the so-called double field method, proposed by Hanle [1]. This method makes it possible to change the electron speeds without a considerable change in the intensity of the electron flow where the excitation of atoms takes place.

In the works carried out to the present, measurement of the intensity of spectral lines was carried out by the basic method of photographic photometry. It was found that, with few exceptions, the excitation functions of the lines have one more or less sharply defined maximum, which is horizontal at an energy of the accelerating electrons somewhat larger than the energy of excitation. On the basis of this fact, it was concluded that the cascade transitions do not play an important role during the excitation of most of the lines, and, consequently, in most cases, the optical excitation function coincides with the excitation function of the energy level which results during the emission of a given line. Up to now, this conclusion was generally accepted. However an analysis of the excitation conditions of the spectral lines causes doubt.

Let us analyze the excitation conditions of atoms during electron collision. Let a beam of electrons penetrate a layer of gas in which the electrons undergo no more than one collision and excite the gas only as a result of collisions with normal atoms. Then the number of excitation events of a given (k) level during collisions with electrons whose velocities lie in a given interval v, v + dv, can be expressed as:

$$dN_k = N_0 Q_{0k}(v)\, N_e F(v)\, dv, \qquad (1)$$

where $N_0$ is the number of atoms arriving on a unit area of the gas layer penetrated by the beam of electrons; $N_e$ is the number of electrons passing through a unit of the cross section per unit time; $F(v)$ is the function of electron distribution with respect to velocities; $Q_{0k}(v)$ is the value which determines the probability of excitation and which is dependent on the electron velocities v. The product $N_e F(v)\, dv$ is the number of electrons whose velocities are included in the given interval v, v + dv. With a monokinetic beam of electrons $F(v) = \text{const}$ and $dN_e = N_e F(v)\, dv$ is the whole number of electrons passing through a unit of cross section per unit time. In this case, the number of excitation events of the k level is written in the following form:

$$dN_k = N_0 Q_{0k}(v)\, dN_e. \qquad (2)$$

In expression (2), $dN_k$ has the dimensions $L^{-2}T^{-1}$; $dN_e$ -- the dimensions $L^{-2}T^{-1}$; $N_0$ -- the dimension $L^{-2}$, and therefore, $Q_{0k}(v)$ will have the dimension $L^2$, i.e., the dimensions of an area, and will be the effective excitation cross section of one atom $\pi r^2$.

We can represent $Q_{0k}(v)$ in the form $Q_{0k\,max} \cdot f(v)$, where $Q_{0k\,max}$ is the effective cross section in the maximum, and f(v) is a certain dimensionless function of v, which is normalized so that it has the value $f(v) = 1$ in the excitation maximum. We will call f(v) the <u>excitation function of the k energy level.</u>

With a non-monokinetic electron beam, it is necessary to integrate the right side of expression (1) with respect to all velocities, beginning with the velocity $v_{0k}$, which is the velocity of the electrons whose energy corresponds to an excitation potential of the k level (critical velocity). Then we will get

$$\Delta N_k = N_0 N_e \int_{v_{0k}}^{\infty} Q_{0k}(v)\, F(v)\, dv. \qquad (3)$$

Up to now we assumed that there were no stepped excitation and cascade transitions. If they do take place, it is necessary to calculate the additional number of excitation acts of a given level which are caused by these processes. This can be done, if we replace expression (3) by the following:

$$\Delta N_k = N_e \sum_{l=0}^{k-1} N_l \int_{v_{lk}}^{\infty} Q_{lk}(v)\, F(v)\, dv + \sum_{i=k+1}^{\infty} N_i\, A_{ik}, \qquad (4)$$

where $A_{ik}$ is the probability of transitions from upper levels to the given one.

Let us now show how it is possible to connect the number of excitation acts with the intensity of the lines for which the given level is the original. In the absence of reabsorption, the intensity of the line corresponding to the transition k→i is determined from the relationship:

$$I \sim N_k\, A_{kl} h\nu_{kl}, \qquad (5)$$

where $N_k$ is the number of atoms in a given k state; $A_{ki}$ is the probability of the transition k → i; $h\nu_{ki}$ -- is the light quantum corresponding to the transition k → i.

The number $N_k$ can be determined from the condition of stationarity: the number of excitation acts is equal to the number of disintegration acts of the given level. If excitation takes place only because of electron collision, and the absorption of light and if the induced transitions and impacts of the second type are absent, the condition of stationarity can be written as:

$$\Delta N_k = \sum_{l=0}^{k-1} N_k A_{kl}. \qquad (6)$$

Since all the $A_{ki}$ are constant, it follows from this equality that for every line originating during the transition from the given level, the intensity I, according to (5), is proportional to $\Delta N_k$. And this means that the relationship between the intensity of the line and the electron velocity will reproduce the relationship between the number of excitation acts and the electron speed. Then, keeping (4) in mind, we can write

$$I \sim N_e \sum_{i=0}^{k-1} N_i \int_{v_{ik}}^{\infty} Q_{ik}(v) F(v) dv + \sum_{i=k+1}^{\infty} N_i A_{ik}. \qquad (7)$$

Thus, the excitation function can be connected with the number of excitation acts of a given level (expression 4), and with the intensity of the lines corresponding to the transitions from this level (expression 7). Hence, we, naturally, arrive at two methods of experimental investigation of the excitation functions-electric and optic.

The electric method is based on the measurement of the distribution of electrons with respect to velocities after they have experienced a non-elastic collision with the atoms. Since this method was not used in the given work, we will not examine it in detail.

The optical method is based on the application of equality (7). Each $N_i$ entering equality (7) is determined in the absence of collisions of the second type by the condition of stationarity (6), which we represent in the form

$$N_e \sum_{i=0}^{k-1} N_i \int_{v_{ik}}^{\infty} Q_{ik}(v) F(v) dv + \sum_{i=k+1}^{\infty} N_i A_{ik} = \sum_{i=0}^{k-1} N_k A_{ki}. \qquad (8)$$

In practice, the application of expressions (7) and (8) is impossible.

When there is a low concentration of excited atoms ($N_i \ll N_0$), we can disregard the stepped excitation. In this case when there is a monokinetic state of the electron beam, formulas (7) and (8) change to

$$I \sim N_0 Q_{0k}(v) dN_e(v) + \sum_{i=k+1}^{\infty} N_i A_{ik} \qquad (9)$$

and

$$N_0 Q_{0k}(v)\, dN_e(v) + \sum_{i=k+1}^{\infty} N_i A_{ik} = \sum_{i=0}^{k-1} N_k A_{ki}. \qquad (10)$$

Both terms on the left in equality (10) can be of the same order. Therefore it is impossible to disregard the term in expression (9) $\sum_{i=k+1}^{\infty} N_i A_{ik}$ (i. e., the role of the cascade transitions). This term vanishes only for the interval of the electron velocities $v_{0k} < v < v_{0,\ k+1}$.

Thus, the intensity of the line, measured as the function of the velocity of the atoms exciting the cross section of gas, will not reproduce the excitation function of the original level. It will represent only a certain summed excitation function, consisting of the excitation function of the original level of the given line and from the excitation functions of those levels from which cascade transitions to the given level are possible. This summed function is called the excitation function of a spectral line, or the optical excitation function. The excitation function of a line, unlike the excitation function of a level, has no direct physical significance.

The fact that the role of cascade transitions has not been revealed until recently is explained by the insufficiencies of previous experiments.

The purpose of our work is to reveal the role of cascade transitions, having imporved the construction of an excitation tube and used the photoelectric method to study the excitation functions of the lines of a visible mercury spectrum.

## 2. The Experimental Instrument

The experimental instrument consists of three parts: 1) tubes which excite a cross section of mercury vapors by an electron beam of given velocity, 2) a monochromator 3) a photoelectric photometer.

Hanle's apparatus [1] was taken as model for our tube. At first, we tested several tube variants to explain the different problems connected with the operation of the tube. We particularly tried to obtain the tube with the best stability of electron emission from the oxide cathode and with the best possible electron monokinetic state in the studied volume of gas. A series of tests led to the satisfactory solution of this problem. We also worked out the technology of the production of excitation tubes with a long life span.

Work on the study of the optical excitation functions of mercury was made in two variants of the excitation tube. A cross section of the second variant is shown in figure 1.

Cylinder 1 made of molybdenum glass is 6 cm in diameter and 50 cm long. In the lower part, it has a spherical expansion and then changes into a narrow tube, 2 cm in diameter. The lower end of tube 2, where liquid mercury is placed, is bent to a $45^{\circ}$ angle with respect to the axes of the tube so that studies can be made when the tube is in vertical and horizontal positions. In glass jaw 3, we fused six inlets made of molybdenum wire on which all the metal parts of the tube were securely mounted. On the side one more inlet was fused, made of fine molybdenum wire. Flask 4 with two inlets was fused onto the side of the tube, in which the getter is atomized. Aperture 5 (figure 1 only shows its projection) was constructed to discharge radiation into the entrance aperture of the monochromator.

The apparatus for receiving the electron beam consisted of the following parts: cathode K, the stretching anode $A_{stretch}$, the regulating anode $A_{reg}$, the guard cylinder $A_{guard}$, and the electron receiver R. All the given components are made of a nickel-tin alloy.

The cathode is a disk 1.55 mm in diameter to which the concave surface is lightly attached (for focusing the emitted electrons). Approximately in the center, the disc is fused on by spot welding to the delicate tungsten wire whose ends are joined to the inlets. Before welding the jaw onto the tube, the surface of the disc is washed with hydrochloric acid, after which

it is boiled in distilled water and, finally, it is carefully washed in carbon tetrachloride [2]. After this, a fine layer of an oxide mixture, dissolved in acetone, is deposited.

The stretching anode is a cylinder covered with the disc on one side. In the disc, along the axes of the cylinder, there is an aperture made in such a way that a tube flange about 2 mm in diameter with flat partitions is obtained. In our opinion, such an aperture distorts the monokinetic state of the electron beam, leaving it considerably smaller than does a simple aperture with sharp edges.

The regulating anode is also a cylinder with a disc. It has an aperture with the same tube flange as the previous anode. The potential of the regulating anode gave the velocity necessary for the electron beam. The guard cylinder of the receiver on the side which faces the anodes had an aperture 10 mm in diameter, covered with a net of nickel wiring with large meshes. Practically the entire electron beam passed through the central mesh. On the opposite side there was an aperture 7 mm in diameter through which a rod passed which served as the exit from the R receiver.

The electron receiver was a cylinder covered at the bottom with a disc. On top it has an aperture for the electrons to pass into it. Inside receiver R we placed nets of nickel wiring with close-woven meshes for retaining the secondary and reflected electrons in the receiver. The receiver was placed in a guard cylinder, and was attached to it with quartz wires. The exit from the electron receiver was carefully protected by a glass insulation from extraneous atoms falling upon it.

All the electrodes were placed in relation to each other at the following distances (with respect to the axes of the instrument): cathode-stretching anode-4 mm; stretching anode-regulating anode-4 mm; regulating anode-guard cylinder-9 mm; guard cylinder-electron receiver-2 mm.

Thus, the observed electron beam was about 9 mm long; the entire length of the electron path (to the guard cylinder) was 17 mm.

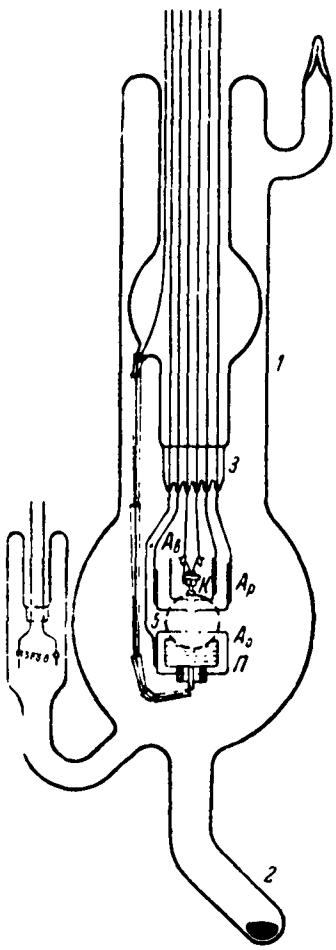


Figure 1. Excitation tube.

Figure 2 gives the electrical lay-out of the instrument. Voltmeters $V_1$ and $V_2$, which have a large range make it possible to easily fix the variations of the accelerating electron potential to 0.1 volts. The current is also recorded with satisfactory accuracy on the receiver by microammeter G.

In the first tube, the construction and geometric dimensions of the electrodes are different from the given one.

Before welding the jaw to the tube, all the components were carefully washed, whereupon the flask which has a getter placed in it, is welded to the tube. After this, the tube is joined to a vacuum apparatus, and pumped out. The tube is pre-aged in a few days. It is housed in a continuous pump, and the tube is simultaneously heated to 400-450°C toward the end of the pre-aging, the mercury is sublimated from a container which was first welded to the bottom part of the tube.

Further, the cathode is activated. It consists in feeding the filament current to the cathode for several minutes, whereupon it is overheated for a short time. The alternation was repeated many times. Then different potentials are fed to the stretching anode and a considerable electron current is obtained from the cathode. The change in the potential at both anodes causes the electron bombardment of the surface of the metal near the apertures and on the meshes for the best degasification of the operating parts. The activating process is accompanied by the continuous pumping of the tube and by its heating to 200°C. Finally, the tube is disconnected from the vacuum apparatus, and the getter is atomized on the flask wall.

The tube prepared in this fashion worked for many tens of hours without any damage to the vacuum and without any noticeable changes in the emissive properties of the cathode.

The luminescence leaving the window of the tube was gathered by a condenser lens on the entrance slit of the monochromator. A glass MS-3 monochromator made by the NIFI LGU works was used as the monochromator. The average dispersion of the monochromator was 70 Å mm. There was enough dispersion with the narrow entrance slit to separate any lines in the visible part of the mercury spectrum. The photomultiplier of the photometer was immediately behind the entrance slit.

The photometer was built at the NIFI LGU experimental works according to the design of S. F. Rodionov, A. L. Osherovich and their associates [3]. A photomultiplier with an aluminum antimonate photocathode was used in the work.

The distance from the entrance slit to the photocathode did not exceed 40 mm. The aperture was bound by a bond 5 mm high, and its greatest width was 0.4 mm. Under these conditions, the luminescence of the light beam in the plane of the photocathode did not exceed the dimensions of the light sensitive surface of the photocathode; therefore there was no need for a collecting lens.

### 3. Measurements and their Results

As we pointed out in the first section, we can experimentally derive the optical excitation function without any distortions if certain conditions are fulfilled. Such conditions are:

1. the absence of reabsorption and second type collisions in the investigated gas or vapor.

2. the absence of step excitations

3. the presence of the monokinetic state of the beam of exciting electrons.

We are not saying here that when there is excitation by an electron collision, frequent collisions should be absent, since in the opposite case the excitation function itself loses its meaning.

The criterion for the fulfillment of the first condition is the linear dependence of the line of intensity on the gas or vapor pressure, and the criterion for the fulfillment of the second condition is the linear dependence of intensity on the flux density.

The criterion for the fulfillment of the third condition should be especially verified from the distribution curve of the electrons according to velocities (energies). The distribution curve is derived by differentiating (graphically) the curve of the voltampere characteristics with retarding potential.

The lower the pressure of the investigated gas or vapor, and the smaller the density of the electron current, the more reliable will be the fulfillment of the first two conditions. Moreover, the luminosity of the luminescent volume of gas decreases rapidly. Therefore, we can decrease the gas pressure and flux density only to those values, which the sensitivity of the apparatus measuring the radiation allows. The inadequate sensitivity of the recording device thus can hinder the creation of the purest experimental conditions. This is the first difficulty in carrying out the experiment.

The second difficulty is the practical impossibility of completely obtaining a monokinetic electron beam. The electrons emitted by the equipotential cathode already have different velocities, caused by the heating of the cathode, the distribution of which is governed in practice by Maxwellian law. The presence of many diaphragms in the path of the beam whose borders cause the partial scattering and reflection of the electrons, and spatial charges -- all aids the increase in the heterogeneity of the electrons with respect to their velocities (energies). On the whole, the energetic heterogeneity of the electron beam can reach several electron volts.

It is obvious that the degree of the monokinetic state of a beam will determine the degree of the approximation of the excitation functions derived from the experiment to the true excitation functions (these functions are certainly not distorted by any other factors). The non-monokinetic state of the electron beam will lead to a great distortion of the optical excitation function. Therefore we consider necessary not only controlling the linearity of the intensity from the gas pressure and flux density but also drawing curves of the distribution of electrons with respect to velocities obtained under the working conditions of the experiment.

Figures 3 and 4 show the relationship between the intensity of several mercury lines and the vapor pressure and the force of the electron current. As these figures show, the linearity is preserved up to $3.5 \cdot 10^{-3}$ mm of Hg vapor pressure (with a constant current density of $0.8 \cdot 10^{-3}$ a/cm$^2$) and to

a current of 100-120 μa (with a constant vapor pressure of $1.3 \cdot 10^{-3}$ mm Hg). A flux density of $4 \cdot 10^{-3}$ a/cm$^2$ (emanating from the aperture area of the regulating anode, it is equal to 0.032 cm$^2$ in the second tube) corresponds to such a current.

Figure 5 shows the curve of the relationship between the current to the receiver and the retarding potential with an initial electron velocity of 12.7 ev. The corresponding differential curve is also given which gives the distribution of electrons with respect to velocities. As the figure shows, about 90% of the electrons have velocities within the interval 1.0 ev. The conditions for obtaining the beam correspond to ordinary work conditions ($V_B$ = 80 v; p = $1.0 \cdot 10^{-3}$ mm Hg; j = $1.0 \cdot 10^{-3}$ a/cm$^2$).

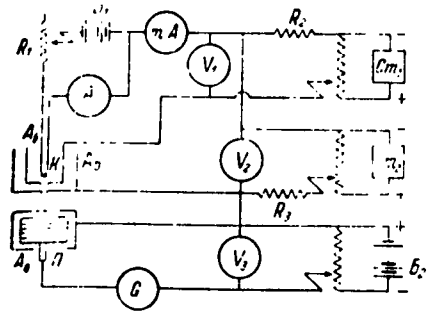

Fig. 2. Electrical set-up of the tube

By decreasing the stretching potential, the current density, and gas pressure (or even one of these factors), we can improve the monokinetic state of the beam. However, a simultaneous decrease in brightness limits this improvement. As we shall show later, we succeeded, when measuring the excitation function of the Hg line, λ 5461 in achieving such a degree of the monokinetic state when about 90% of the electrons had velocities in the limits of 0.5 ev.

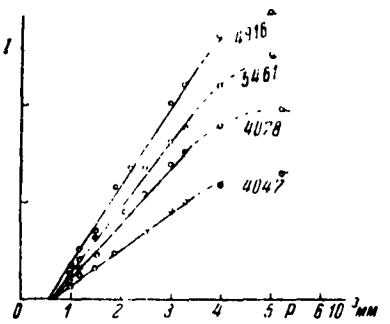


Fig. 3. Relationship between line intensity and pressure

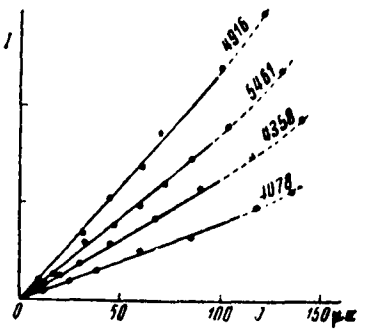


Fig. 4. Relationship between line intensity and current.

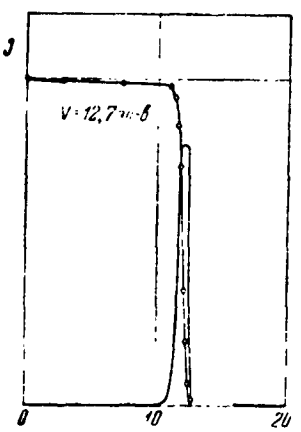


Fig. 5. Distribution of electrons with respect to velocities

When studying the excitation functions, the purity of the investigated vapor which was verified spectroscopically, is very important. No traces of extraneous lines, except Hg lines, were revealed.

Other control measurements have revealed the absence of any influence of scattered light in the monochromator on the results of the measurements, and also the absence of any noticeable heterogeneties in the structure of the electron beam under usual work conditions.

Finally, we verified the linearity of the curves of the photoelectric photometer. Special measurements have shown that in the work regime of the photometer which we used, the relationship between the photocurrent and the light flux was linear with an error that does not exceed 4%.

The given experimental material was obtained while working on two excitation tubes. The differences in the geometric characteristics of the

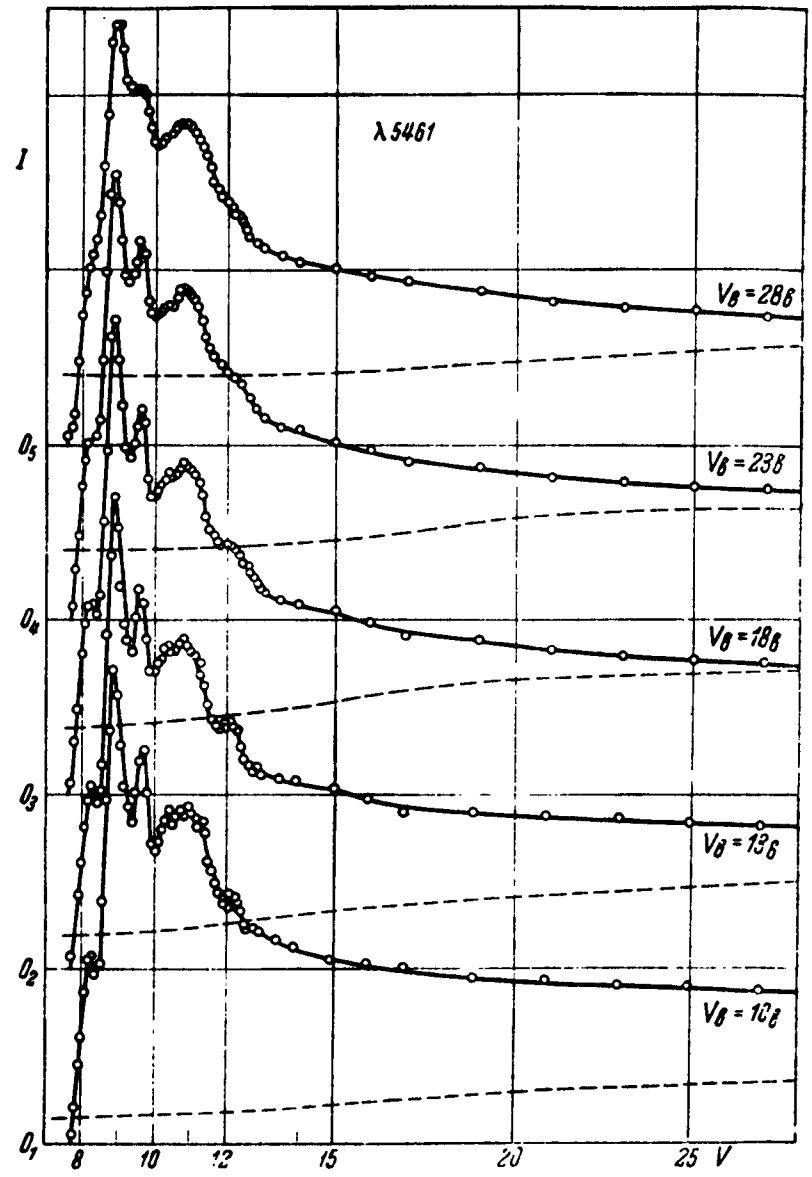


Fig. 6. Excitation function of the mercury line λ5461.

tubes are not at all visible in the results of the measurements, at least in that region of vapor pressures and electron current densities in which all our basic measurements were made.

The object of our investigation was eight lines of the visible mercury spectrum. Six lines were repeatedly and carefully measured: λλ 5461 ($6^3P_2$ - $7^3S_1$), 4358 ($6^3P_1$ - $7^3S_1$), 4047 ($6^3P_0$ - $7^3S_1$), 4108 ($6^1P_1$ - $S_0$), 4916 ($6^1P_1$ - $8^1S_0$), and 4078 ($6^3P_1$ - $7^1S_0$). We determined that the excitation functions of these lines have a thin structure. The excitation functions of two lines of a diffused series λλ 4347 ($6^1P_1$ - $7^1D_2$) and 5791 ($6^1P_1$ - $6^1D_2$) did not reveal a thin structure; therefore they were studied in less detail.

When determining excitation functions, the measured potentials did not correspond to the actual electron velocities due to the presence of a contact difference of the potentials between the cathode and stretching anode, and also due to the decrease in potential at the one half of the heater filament, through which the voltmeter is joined to the equipotential cathode. Since our graphs give a rather accurate description of the moment when the excitation function increases sharply, the intersection of the beginning part of the excitation function with the abscissa should accurately (up to 0.1 volts) give the beginning of the excitation of a given line. The necessary correction is found by subtracting the excitation potential, calculated from the energy of the upper level of the line, from the value of the voltmeter at which the excitation of the given line begins. This correction is the same for all the lines and under the usual conditions of our measurements was approximately equal to 2.3 volts.

The excitation functions of the lines of the triplet λλ 5461, 4358, and 4047 are completely the same. Therefore, we did not have to give them separately for the three lines. Figure 6 shows the excitation functions of the line λ5461 obtained during different stretching potentials. The function has three potentials somewhat larger than the critical, a series of maxima. The better these maxima are solved, the less the stretching potential.

The excitation functions of lines λλ 4108, 4916, 4078, and λλ 4347, 5791 are shown in figures 7 and 8. All the excitation functions are measured under the same vapor pressures ($p = 1 \cdot 10^{-3}$ mm Hg), the same current density ($0.5 \cdot 10^{-3}$ a/cm$^2$) and other excitation conditions. The points on the curves where the maxima are located were taken to 0.1 volt.

Table 1 gives the number and position of the maxima of the investigated eight lines of the visible mercury spectrum.

TABLE 1

| Wave length λ в A | Serial Symbol | Excitation potential (in ev.) | Number of Observed Maxima (in volts) | position of observed maxima (in volts) |
|---|---|---|---|---|
| 5461 | $6^3P_2-7^3S_1$ | 7,69 | 6 | 8,2; 8,9; 9,6; 10,5; 11,0; 12,4 |
| 4358 | $6^3P_1-7^3S_1$ | 7,69 | 6 | To же |
| 4047 | $6^3P_0-7^3S_1$ | 7,69 | 6 | To же |
| 4078 | $6^3P_1-7^1S_0$ | 7,90 | 4(+1)[1] | 8,7; 10,0; 11,1; 13,1 (~30) |
| 4916 | $6^1P_1-8^1S_0$ | 9,18 | 2(+1) | 10,2; 11,1; (~35) |
| 4108 | $6^1P_1-9^1S_0$ | 9,67 | 2(+1) | 10,4; 11,1; (~35) |
| 5791 | $6^1P_1-6^1D_2$ | 8,80 | 1(?) | 18 |
| 4347 | $6^1P_1-7^1D_2$ | 9,51 | 1(?) | 20 |

Lines λλ4078, 4916 and 4108, besides the maxima close to the excitation potential, also have a very wide and flat maximum at electron velocities of 30-35 ev. Other authors noted this maximum [4]. As far as the series of maxima near the excitation potential on the first 6 lines are concerned, they were formerly not determined and for the first time they were reliably projected on our curves. The excitation functions of the lines λλ4347 and 5791 did not reveal any separate sharp maxima.

---

1. The brackets denote the plane maxima which are in the region of the high energies of the exciting electrons.

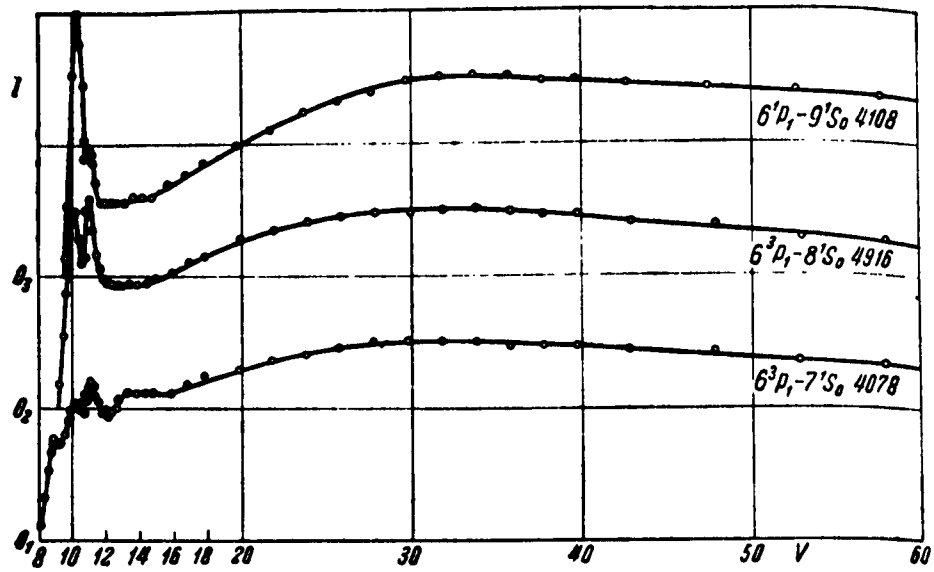


Fig. 7. Excitation functions of the mercury lines λλ 4108, 4916, and 4078.


Fig. 8. Excitation functions of the mercury lines 4347 and 5791.

Since the current to the receiver increased somewhat (sometimes to 1.5 times) when the velocity of the electrons increased, beginning from the excitation potential of the lines (7.7 - 9.7 volts to 60 ev, the line intensity for each measured value of the velocity of the exciting electrons is transferred to the same current. The relationship between the current to the receiver and the velocity of the exciting electrons gives a completely smooth curve (the dotted curves in figure 6) without hint of any jumps. The current is estimated both when measuring the relative intensities of the lines, for each 0.2 volts, and in more accurate measurements -- for 0.1 volt. Thus, there is no basis to suspect the appearance of certain maxima because of a sudden increase in current in the excitation functions which we derived.

### 4. Control Experiments

The curves shown in figures 6, 7, and 8 were obtained when the tube was so situated that the luminescent column of gas was perpendicular to the aperture of the monochromator which cut out a section along the entire width of the column. In such a case, the photometer integrated the intensity of the luminescent column along its entire width. This made it possible to avoid errors due to a change in the geometric measurements of the column, which could change because of different focusing.

When the luminescent column is parallel to the aperture, we succeeded in realizing considerably greater light fluxes on the photocathode than when it was perpendicular. Observations have shown that no essential distortions in the curves result because of this.

Therefore, we investigated the following with respect to their effect on the excitation function: a) the magnitudes of the stretching potential b) vapor pressure, c) current density, d) the degree of the monokinetic state of the electron beam when the excitation tube was so positioned that the luminescent column was projected along the entire length to the aperture of the monochromator.

Figure 9 shows the excitation functions of the line λ 4078 obtained under the conditions only when the stretching potential changes from 90 to 30 volts. As this figure shows, the change in the stretching potential somewhat distorts the curves, but this distortion is noticeable only in a region which is far from the excitation potential.

This distortion is easily explained by the fact that with different stretching potentials the beam in the observed volume of gas is focused somewhat differently, and this leads to a certain change in the current density in the beam. It is most noteworthy that the region of fine structure immediately behind the excitation potential preserves its form when there are different values of the stretching potential.

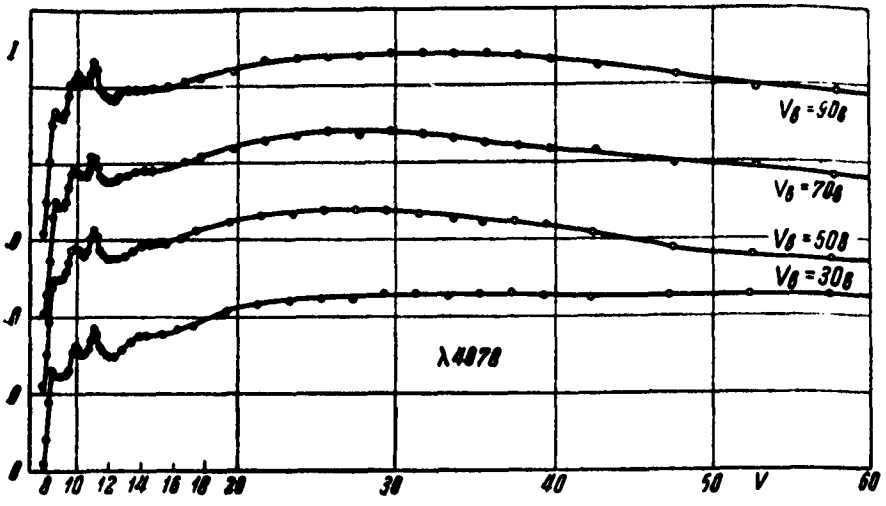


Fig. 9. Excitation functions of line λ4078 when there are different stretching potentials.

During the measurements, the results of which are shown in figure 6, the stretching potential varied in the interval of small values - from 28 to 10 volts (the latter value is less than the ionization potential of Hg vapor). However even here there are no deviations from the properties of the obtained structure for lines of the visible triplet of mercury.

This figure shows that when there is a decrease in the stretching potential, the separate components of the thin structure of the excitation function is solved even easier. A change from 90 to 30 volts in the stretching potential almost has no effect on the form of the curve in the region where the maxima of the thin structure are located. The reason is that in the region of the small values of the stretching potentials (especially when there are very low vapor pressures and small current densities) the monokinetic state of the beam of exciting electrons improves very noticeably. This is shown in figure 10 from which it follows that with a change from 80 to 30 volts in the stretching potential, the monokinetic state of the electrons remains the same (about 90% in the 2-volt region) and with a further decrease to 13 volts, it improves considerably (about 90% of the electrons are in the 1.5 - volt region).

Let us note that with a decrease in the stretching potential, approximately beginning at 30 volts, it becomes all the more necessary to increase the filament current of the oxide cathode in order to obtain an electron current of sufficient magnitude.

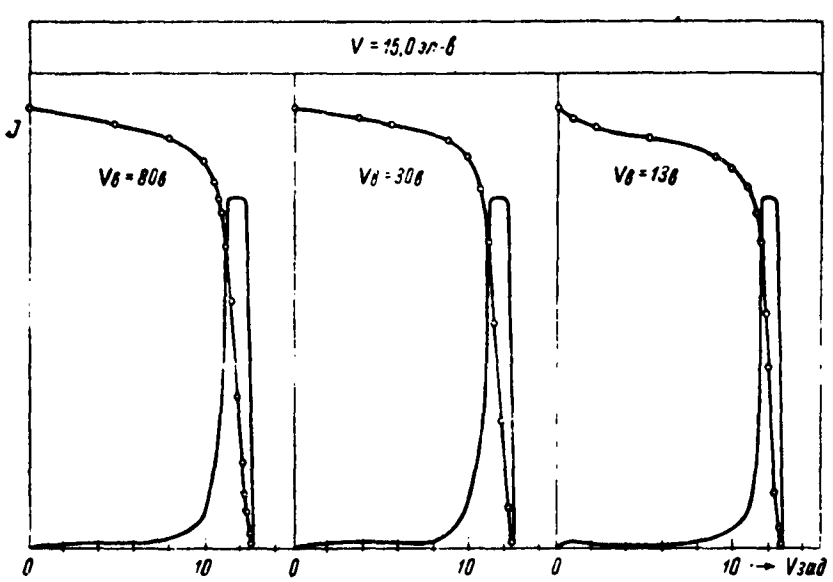


Fig. 10. Distribution of electrons with respect to velocity when there are different stretching potentials

The behavior of the excitation functions when there is a change in vapor pressure is shown in figure 11. For all the curves of this figure, all the conditions except that of pressure, are the same. The current density is approximately equal to $0.5 \cdot 10^{-3}$ a/cm$^2$; the region of pressure change is from $1 \cdot 10^{-3}$ to $5 \cdot 10^{-3}$ mm of Hg. We can also see from the figure that in the limits of the pressure change from $1 \cdot 10^{-3}$ to $3 \cdot 10^{-3}$ mm Hg, the curves are rather similar. With a further pressure increase, the curves begin to change noticeably. Such a behavior of the curves agrees well with the linear dependence of the intensity on pressure in the interval from $1 \cdot 10^{-3}$ to $3 \cdot 10^{-3}$ mm Hg, and with the fact that with these pressures, the free path length of the electrons (9-3 cm) is greater than the total electron path in the tube (1.8 cm). With a further pressure increase, the free path length becomes equal to or less than the total electron path. In this case, a significant role will be played by double and multiple collisions which cause distortions in the correct path of the excitation function.

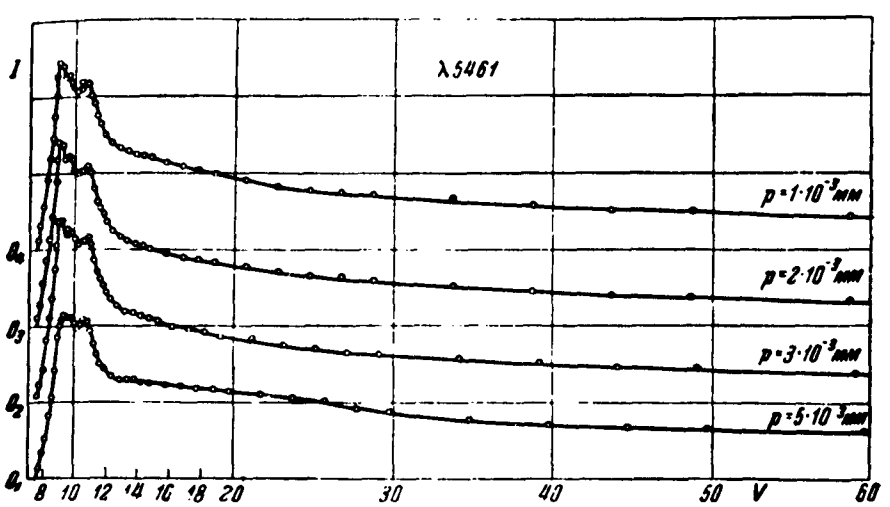


Fig. 11. The excitation function of line λ5461 under different vapor pressures of mercury

The effect of the change in the current density on the behavior of the excitation function is shown in figure 12. The remaining conditions are the same for all the curves of this figure. The current changed more than 4 times -- from 30 to 130 μA (which corresponds to the change in current density from $1 \cdot 10^{-3}$ to $4 \cdot 10^{-3}$ a/cm$^2$). In this interval of change of the current density, as the figure shows, the nature of the curves are fully preserved. Some deterioration in the solution of maxima of a thin structure, noticeable in the excitation function of λ 4078 during considerable current densities, and also a certain converging of the maxima are caused by the fact that when there are considerable current densities, an intense focusing of the beam takes place, and with even greater densities, there is a negative spatial charge. Under these conditions noted by our instruments, the potentials cannot correspond to the actual velocities of the electrons in the beam.

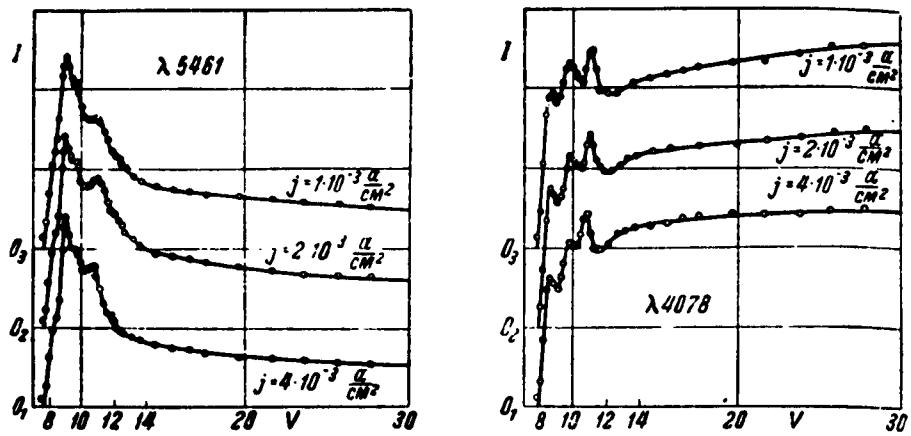


Fig. 12. Excitation function of lines λλ 5461 and 4078 with different current densities.

As we have already pointed out above, a thin structure was not revealed in the excitation functions of the lines of the series $6^1P_1 - n^1D_2$ (λλ 4347 and 5791), although experimental points in the region of velocities immediately after the excitation potential were taken rather often -- to 0. 2 volts.

The smooth nature of the excitation functions of these lines is another proof of the fact that the maxima of a thin structure in the excitation functions of other lines are not caused by anything external in the excitation tube. They, without a doubt, reflect the real nature of the intensity of these lines when there is a change in the velocity of the exciting electrons. The reasons for these maxima will be discussed below.

This article gives only a part of the curves obtained. We measured more than 100 curves. Experimental points were taken in them as often as it was expedient to do so when measuring a given excitation function. Usually experimental points were taken to 0.2 or 0.1 volt in the area located between the beginning of excitation and the sloping parts of the curves. Each curve was drawn through 40-70 experimental points; the voltmeter was accurate to 0.05 volt.

We were able to carry out such a number of measurements only because the photographic method of recording the intensity was replaced by the photoelectric method. Due to the greater sensitivity of the photoelectric photometer in comparison with the photoplate, much less time was required to obtain the excitation functions of any line. The high sensitivity of the photometer made it possible to use lower vapor pressures and current densities, i.e., to make more reliable the conditions necessary for determining excitation functions.

Let us make some comparisons. In the work of Schaffernicht [4], which is considered one of the best works for determining excitation functions by the photographic method, a current density of about $1 \cdot 10^{-3}$ a/cm$^2$ and higher, and a vapor pressure of $3 \cdot 10^{-3}$ mm Hg were used. We made final measurements with current densities of $0.5 \cdot 10^{-3}$ — $1 \cdot 10^{-3}$ a/cm$^2$ and vapor pressures of $1 \cdot 10^{-3}$ -- $1.2 \cdot 10^{-3}$ mm Hg, and in a series of measurements we obtained a current density of $0.1 \cdot 10^{-3}$ -- $0.2 \cdot 10^{-3}$ a/cm$^2$, and vapor pressures of $0.8 \cdot 10^{-3}$ mm Hg. Thereupon, the intensity decreased so much that the use of the photographic method would actually have been impossible. When there were such low current densities and low vapor pressures, we were able to obtain a good solution of the maxima of the excitation functions of the lines of a visible triplet of mercury.

As the works of many other authors show, with the photographic method, from 2 to 30 minutes are required to obtain one point on the experimental curve for comparatively bright lines, and up to 2 hours for weak lines. To obtain the number of points required to construct the entire excitation function of a line, several hours to a day of continuous work were necessary. Moreover, considerable time was expended on the photometry of photoplates and on the conversion of the blackenings into the relative intensities of the lines. Several seconds were necessary to photometrically determine one experimental point, and 15-30 minutes were required to obtain the number of points (let us say, 70 points) necessary to construct the excitation function, whereupon all the points were determined with maximum accuracy in this case.

During this time the conditions of the experiment were held constant, and the current increased only somewhat (in proportion to the increase of the accelerating potential). Therefore, the only correction which must be made to convert from the directly observed points to the excitation functions of the line, is this transfer of the intensities to one point.

The speed in determining experimental points makes it possible to verify with great accuracy any portions of the excitation functions including their beginning part which is most important.

We made special measurements to determine the convergence of separate measurements and their accuracy. For example, for five different accelerating potentials, which lie in the region of the thin structure (9, 10, 11, 13, and 18 volts), for line $\lambda$ 5461 with a vapor pressure of $p = 1 \cdot \cdot 10^{-3}$ mm Hg and a current density of $j = 0.2 \cdot 10^{-3}$ a/cm$^2$, photocurrents at the exit of the photometer were measured 10 times in succession. The average value was calculated from the ten values for the given accelerating potential. Further, the tube was shut off (the filament current, feeding the anodes, etc.) and thereupon the former conditions were created, and

the measurements were carried out again. Thus, several groups of measurements were obtained. It turned out that deviations from the average value of the photocurrent in each separate group did not exceed 2%, and between the groups -- 3%.

We also verified the frequency of the results for the entire excitation function. Under the same conditions, we measured three times in succession the excitation function of line λ 5461, which includes 70 experimental points (from the excitation potential to 30 ev. ). The largest value of scattering (in relation to the maximum value of intensity) was 2%.

Figure 13 shows two curves of the excitation function of the same line λ 5461, obtained under the same conditions, but with the only difference that one was measured when there was an increase in the accelerating potential, and the other when there was a decrease (the arrows indicate the direction of the potential change). The curves obtained are identical, their maxima coincide with an accuracy of 0.1 volt.

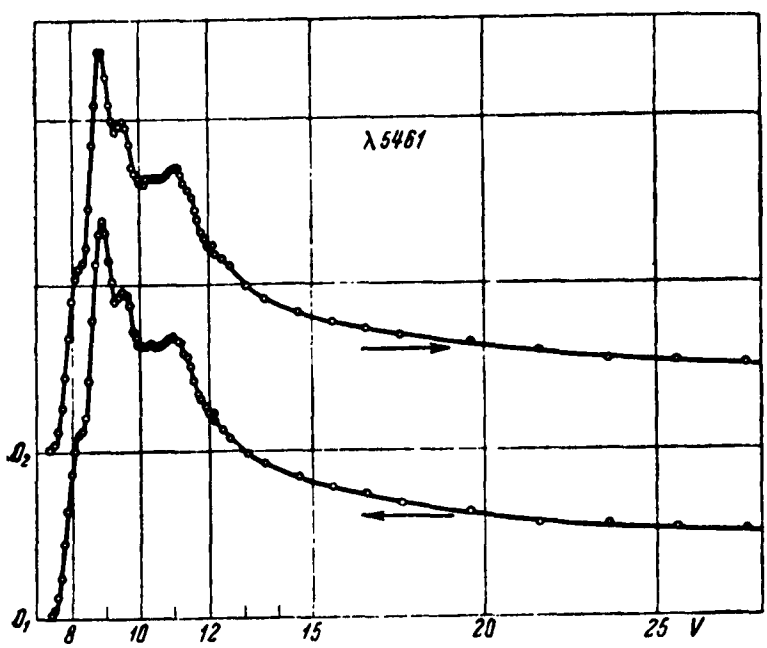


Fig. 13. Comparison of the excitation functions of line λ 5461, obtained when there was a decrease and increase in the accelerating potential.

## 5. The Role of the Monokinetic State of the Beam of Exciting Electrons

As we have noted more than once in this work, it is necessary to consider the degree of the monokinetic state of the electrons in experiments on the determination of the excitation functions. However this problem of the excitation functions has not been covered enough in many works. It was considered that the heterogeneity of electrons with respect to velocities of 2-4 ev does not cause any essential changes in the form of the excitation function. Many authors gave no information at all on the monokinetic state of exciting electrons only indicating that there was somehow a sufficient beam homogeneity.

In order to experimentally confirm how the degree of the monokinetic state of an electron beam effects the form of the specific excitation functions, we made special experiments in which the degree of the homogeneity of a beam deteriorated artificially.

Under ordinary working conditions, we measured the excitation function of a given line and the relationship between the current and the retarding potential when there were the electron velocities in which we were interested. An additional accelerating potential $V_g$ (from 0.5 to several volts) was placed on the electron beam between the regulating anode $A_{reg}$ and the guard cylinder $A_0$ (see figures 1 and 2). This led to an explanation of the accelerating electron field in the region where there was an electron collision with the atoms, i.e., in the region which was assumed equipotential during ordinary experiments. The excitation function and the relationship between the current and retarding potential were again measured without changing any of the other conditions of the experiment. The excitation functions obtained in both cases, and the curves of electron distribution with respect to velocities (energies) computed by differentiation (from the voltampere characteristics) were compared.

A comparison of the obtained curves immediately shows that in the second case (with the superposition of an additional potential), the maxima

of the thin structure of the excitation function were smoothed considerably, and some even disappeared. The electron distribution curve remained, as was to be expected, exactly as it was in the first case, but moved along the energy axes (in the direction of large energies) to a magnitude equal to the additional potential. This happened because of the fact that the electron velocities in the region from $A_p$ to $A_0$ increased to the magnitude of the additional potential.

We made measurements with the additional potential when the tube was so placed that approximately 4/5 of the height of the image of the luminescent gas column (between $A_p$ and $A_0$) passed from the exit aperture to the photocathode of the photomultiplier. Therefore the measured excitation function corresponded to such a degree of non-uniformity of the electron velocities, which was only a little (approximately 20%) less than the non-uniformity caused by the accelerating potential in every part of the region from $A_p$ to $A_0$.

Such measurements were made only for lines λλ 5461, 4916, 4078, and 4047 with both tubes operating, and every time we determined the relationship between the degree of the resolution of the components of the thin structure of the excitation functions and the degree of the monokinetic state of the beam of exciting electrons.

Figure 14 shows the change in the form of the excitation function of line λ 5461 with the consequent deterioration of the homogeneity of the electron beam in the investigated volume of gas in the interval of 0.5 to 3.5 ev (actually, somewhat less). All the curves were derived under the same conditions of vapor pressure ($1 \cdot 10^{-3}$ mm Hg), current density ($0.5 \cdot 10^{-3}$ a/cm$^2$), and retarding potential ($V_b$ = 28 volts). The right portion of the figure shows curves of the electron distribution with respect to velocities with additional potentials from 0 to 3 volts, and for the case $V_g$ = 0-and the voltampere characteristics. The electron velocity without an additional potential was equal to 10 ev, i.e., it corresponded to the middle of the region of the thin structure. The dotted curves show the distribution of

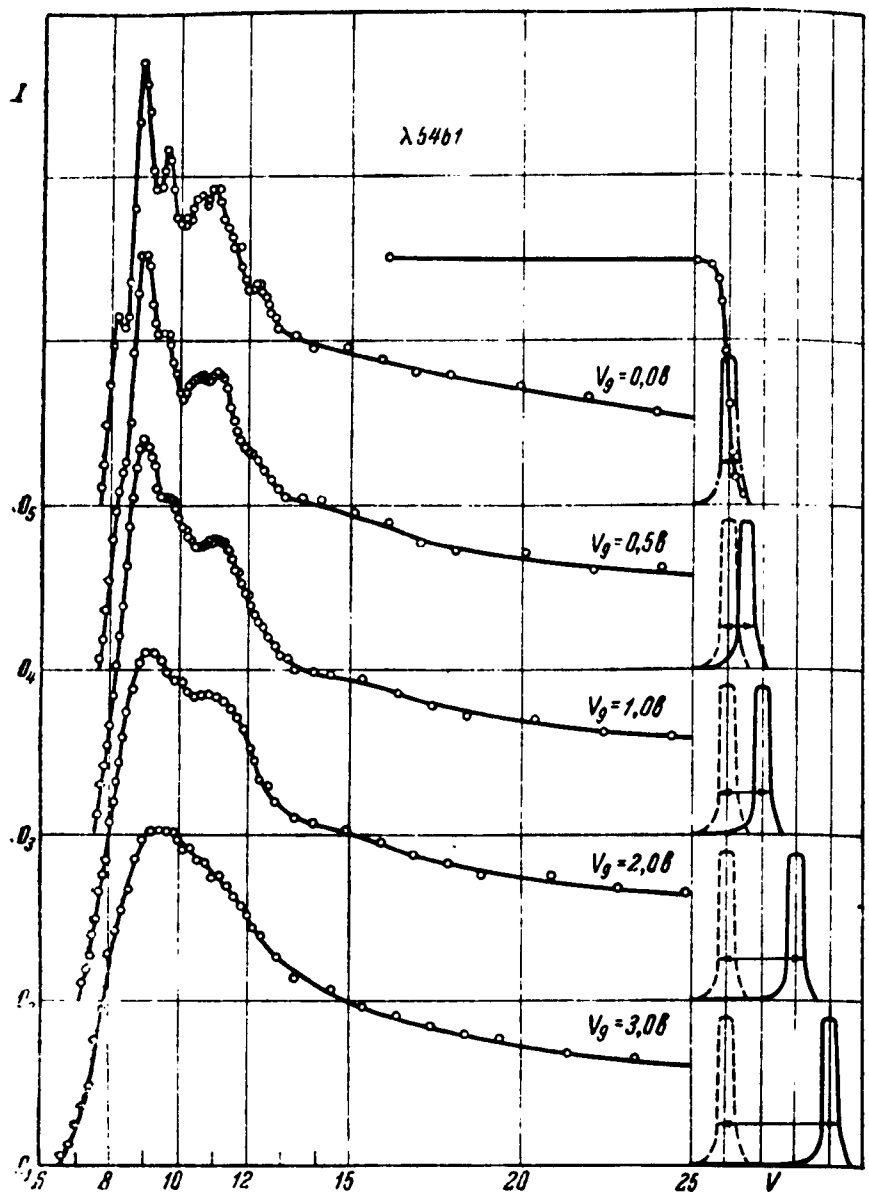


Fig. 14. Effect of the heterogeneity of the electron beam on the form of the excitation function of line λ 5461.

electron velocities in the beam at the retarding anode, and the solid curves at the guard cylinder. The horizontal segments indicate the width of the spread interval of the electrons with respect to their velocities according to the entire height of the beam (from $A_p$ to $A_0$).

When the width of the region of heterogeneity of the beam is 0.5 ev, the excitation function is derived with clearly expressed maxima of the thin structure. With an increase in the heterogeneity of the beam, the separate components of the thin structure gradually smooth out, and thereupon they do not disappear at all (when $V_g$ = 3.5 volts). One relatively wide maximum remains with a rounded apex, similar to the maximum of the excitation function of line λ 5461 which was obtained in the work of Schaffernicht.

The relationship between the degree of the solution of the components of a thin structure and the degree of the monokinetic state of a beam are also shown in figure 15 for the excitation functions of three lines of a visible mercury triplet. But here the deterioration of the monokinetic state (in a comparatively small electron-volt interval) was achieved by adding a supplementary potential, as we did in the former case, but by another method. We recalled that an increase in the retarding potential noticeably deteriorates the monokinetic nature of the electron beam. This was the case for the first as well as the second tube and, obviously, is a property of the construction of the excitation tubes. Moreover, changes in the current density and pressure (in the limits of linearity of the corresponding characteristics) also lead to a change in the monokinetic state of the electrons. An increase in the retarding potential from 15 to 25 volts and an increase in the current density from $0.2 \cdot 10^{-3}$ to $1.0 \cdot 10^{-3}$ a/cm$^2$ (with a pressure of $1.1 \cdot 10^{-3}$ mm Hg) led to a change in the degree of the monokinetic state in the limits of the width of the electron spread with respect to the velocities from 0.5 to 1.1 ev.

The top most triplet to the curves in figure 15 was obtained under the very same conditions which correspond to the width of the interval of heterogeneity of electrons with respect to velocities of 1.1 ev. The average triplet of the curves also derived under the same conditions* corresponds to the

* In this case, the apertures of the monochromator were considerably wider than the aperture when λ 4358 does not overlap its relatively weak neighboring line λ 4347. Therefore, the sloping part of the excitation function of line λ 4358 was elevated a little (due to the neighboring line). Its actual path is shown by the dot.

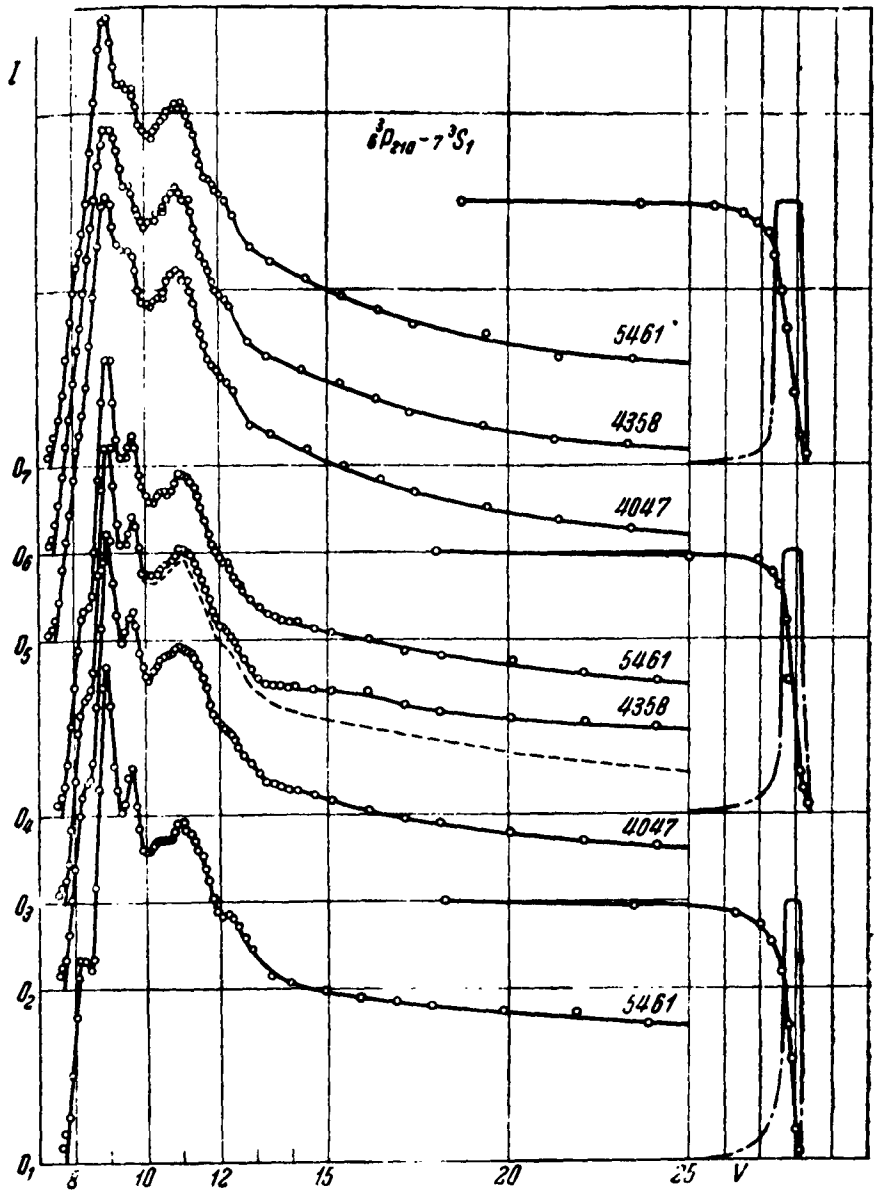


Fig. 15. Effect of the heterogeneity of an electron beam on the form of the excitation functions of lines λλ 5461, 4358, and 4047.

width of the interval of heterogeneity which is approximately 0.8 ev; an interval width of 0.5 ev corresponds to the lowest curve. We were limited to one curve (λ 5461) for the 0.5 ev width of the interval of heterogeneity because of the fact that the remaining lines of the triplet during a small current density ($0.2 \cdot 10^{-3}$ a/cm$^2$ become more difficult to measure.

The relationships between the current and the retarding potential, and the differential curves corresponding to it are shown in the right portion of figure 15 (as in the previous figure). The curves shown in this figure again graphically confirm the effect of the monokinetic state of the electron beam on the form of the optical excitation functions: with an improvement in the degree of the monokinetic state of the beam, the individual maxima of the thin structure are better expressed.

This figure also simultaneously verifies that the excitation functions of a visible mercury triplet completely coincide in the smallest components of the thin structure.

We should note that a further improvement in the monokinetic state of an electron beam can lead to an increase in the accuracy of the form of the curve which represents the optical excitation function of the line. However in all probability this will not at all change the results which we obtained.

We have to especially deteriorate the monokinetic state of the electron beam in order that our excitation functions coincide with the corresponding curves in Schaffernicht's work [4]. Figure 16 shows such a comparison for lines λλ 5461, 4047, 4916, and 4078. The black circles and solid curves in this figure represent the experimental points and excitation functions obtained by Schaffernicht, and the white circles are taken from our excitation functions, obtained when the width of the heterogeneous region of the beam is more than 2 ev. The figure shows that the general path of the curves coincides rather well. *

---

* Schaffernicht erroneously extrapolated the beginning portion (up to the first experimental point) of the excitation function of line λ 4078. As a result all the maxima moved in the direction of the large volts. Therefore for better agreement, we had to move the white circles approximately 0.5 volt.

The dotted curve for λ 4916 was obtained when there was a better monokinetic state of the beam (the width of the interval of heterogeneity was approximately 1. 0 ev). We see that the two maxima of the thin structure of the excitation function of this line are not wider (along the velocity axes) than the width of one maximum of Schaffernicht's curve.

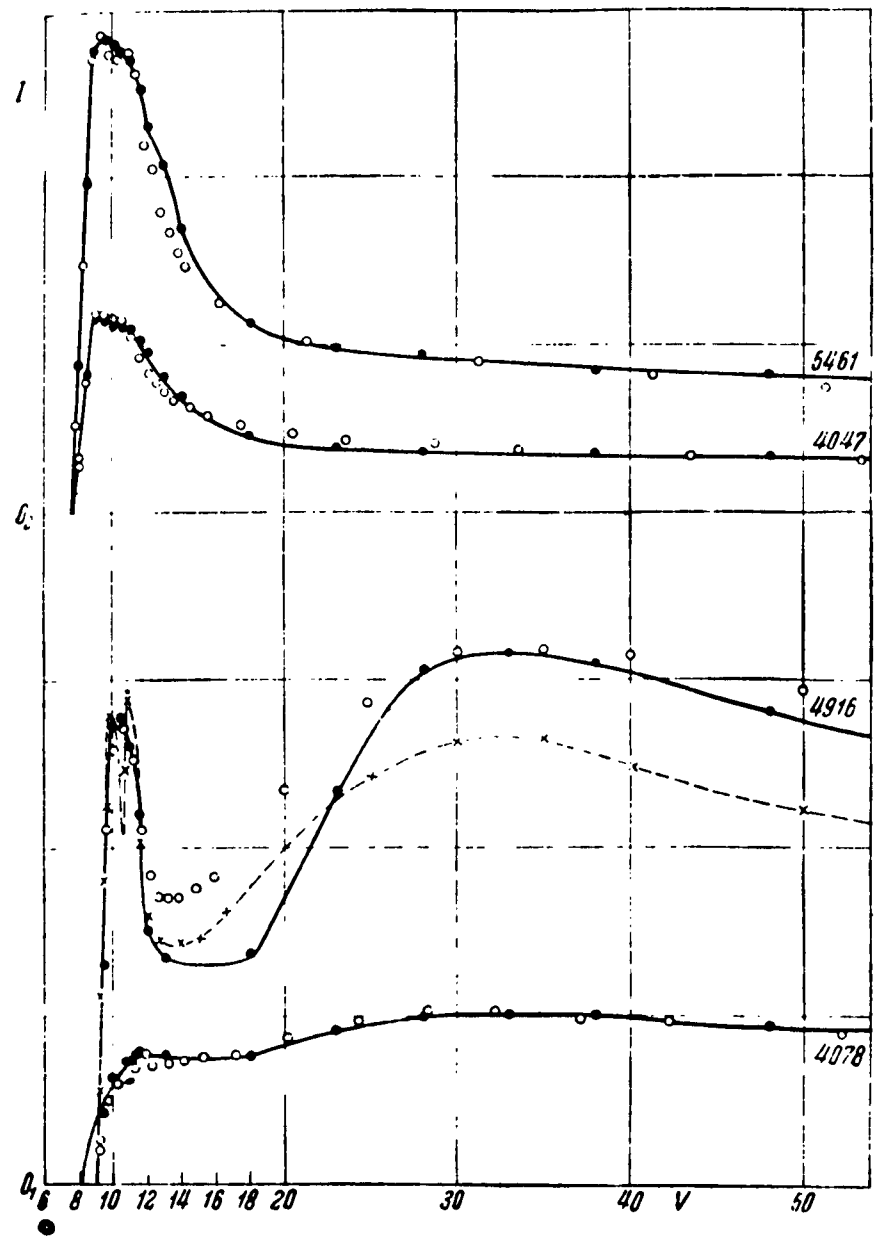


Fig. 16. A comparison of the experimental points obtained by Schaffernicht (the black circles) and by the author (the white circles) when the width of the heterogeneity of the electron beam was 2 ev.

## 6. The Origin of the Thin Structure of the Optical Excitation Functions

The measurements of the excitation functions of six lines of the visible mercury spectrum (λλ 5461, 4358, 4047, 4108, 4916, and 4078) under the most diverse conditions of excitation, and a series of control measurements have shown that these functions undoubtedly possess a structure which we cannot attribute to any chance reasons.

In the first section, we showed that the optical excitation function should consist of the excitation function of the initial level of the line and of the excitation function of higher levels from which cascade transfers to the initial level are possible. This conclusion is fully confirmed by the results of our work. As we have shown in the previous article [5], the maxima of the thin structure of the excitation function of the line are caused by the excitation functions of the individual levels. In order to show that this is actually so, let us examine each optical excitation function separately.

Line λ 5461; the transfer $7^3S_1 \rightarrow 6^3P_2$. The excitation potential of the initial level of the line $7^3S_1$ is equal to, 7.69 volts. Let us see from what levels the cascade transfers to the level $7^3S_1$ are possible.

First, transfers are possible from the triplet levels $n^3P_{012}$ when $n = 7, 8, 9 \ldots$ The excitation potentials for the levels $7^3P_{012}$ are equal respectively to 8.58; 8.59, and 8.78 volts; for the levels $8^3P_{012}$ - 9.43; 9.43 and 9.48 volts; for the levels $9^3P_{012}$ - 9.8; 9.8, and 9.82 volts, etc. These transfers have a considerable probability, especially the transfers from the levels $7^3P_{012}$, from which there are no other intensive transfers except to the $7^3S_1$ level (the intercombined transfer $7^3P_1 \rightarrow 6^1S_0$ is improbable).

Second, transfers from the identical levels $n^1P_1$ are possible when $n = 7, 8 \ldots$ However such intercombined transfers are considerably less possible in comparison to the transfers corresponding to the principal series of identities $n^1P_1 \rightarrow 6^1S_0$, and we can disregard them.

Let us now consider the case that our excitation functions are determined with such a degree of the monokinetic state of the electron beam, when about 90% of the electrons had velocities in the interval, approximately 0.5 ev wide. Therefore the excitation functions of the levels (which can evolve due to the cascade transfers) which are separated from each other by less than 0.4 volt, cannot be observed as completely dissociated. Consequently, the path of the optical excitation function of the line λ 5461 should affect the cascade transfers from the levels $7^3P_{012}$, $8^3P_{012}$, $9^3P_{012}$, and under the conditions of our experiment from the group of insolvable higher levels $n^3P_j$, $n \geq 10$.

Then we can lay out the excitation function of line λ 5461 (and the excitation functions λλ 4358 and 4047 which are analogous to it) on the excitation function of the separate levels approximately as figure 17 shows. The first small maximum on the experimental curve when V = 8.2 ev is caused by the excitation of the initial level $7^3S_1$ by direct electron collisions. The three following maxima-when V = 8.9; 9.6 and 10.5 ev - refer to the excitation of the levels $7^3P_j$, $8^3P_j$, and $9^3P_j$, which have the corresponding excitation potentials of 8.6; 9.4 and 9.7 volts. The fifth maximum-when V = 11 ev - refers to the excitation of the unsolved group of levels $n^3P_j$ when $n \geq 10$. The diffused maximum-about 12.4 ev, in all probability, refers to the process of recombination of the mercury ions with the free forming electrons. Obviously, the role of the cascade transfers, especially from the levels $7^3P_{012}$, is very great. The excitation of the $7^3P_{012}$ levels should be accompanied by the radiation of the infrared triplet λλ 11287, 13673 and 13951 Å, which we could not observe due to the insensitivity of the photoelectric photometer used in this part of the spectrum.

Let us now consider the lines λλ 4078, 4916 and 4108 to which the transfers $7^1S_0 \rightarrow 6^3P_1$, $8^1S_0 \rightarrow 6^1P_1$, and $9^1S_0 \rightarrow 6^1P_1$ correspond. The excitation potentials of the primary levels of these lines $7^1S_0$, $8^1S_0$ and $9^1S_0$ are equal to 7.89; 9.18 and 9.67 volts respectively. At the $7^1S_0$, $8^1S_0$ and $9^1S_0$, cascade transfers are possible from the $n^1P_1$ levels when n = 7, 8, 9... The

excitation potential of level $7^1P_1$ is equal to 8.8 volts, level $8^1P_1$ to 9.72 volts, level $9^1P_1$ to 9.86 volts, level $10^1P_1$ to 10.01 volts, etc. Obviously, the group of levels beginning from the $8^1P_1$ level and higher, cannot be solved from each other under the conditions of our experiment.

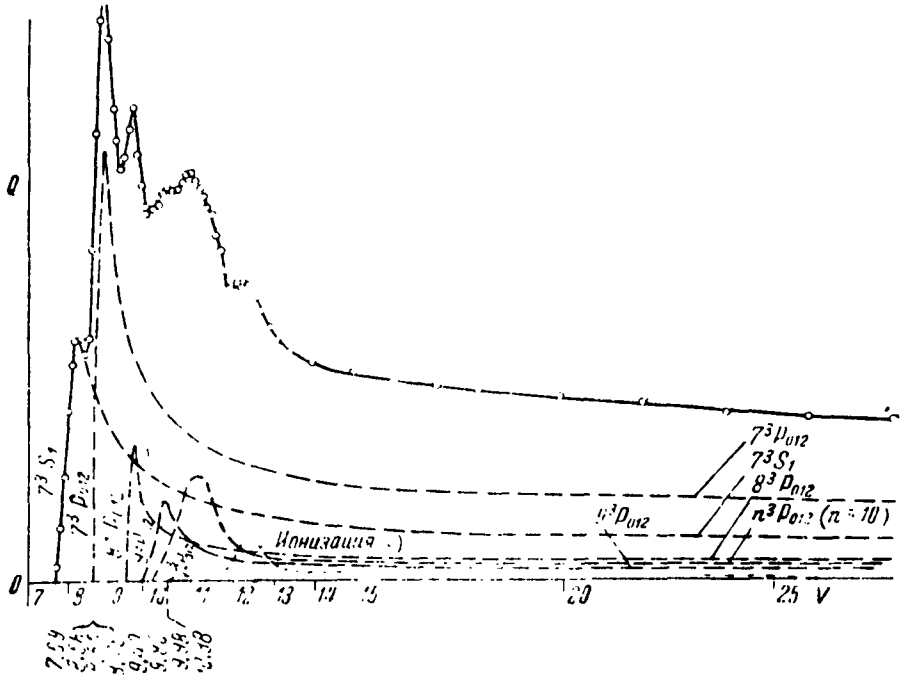


Fig. 17. The dissociation of the excitation function of line λ 5461 in the excitation function of the separate energy levels.

Proceeding from these considerations, the excitation functions of the lines λλ 4078, 4916 and 4108 can be represented as consisting of the excitation functions of the separate levels as shown in figure 18.

The first maxima of the excitation functions of the lines of the visible triplet are caused by the direct excitation by the electrons of the primary levels $7^1S_0$, $8^1S_0$ and $9^1S_0$. The second maximum of the excitation function

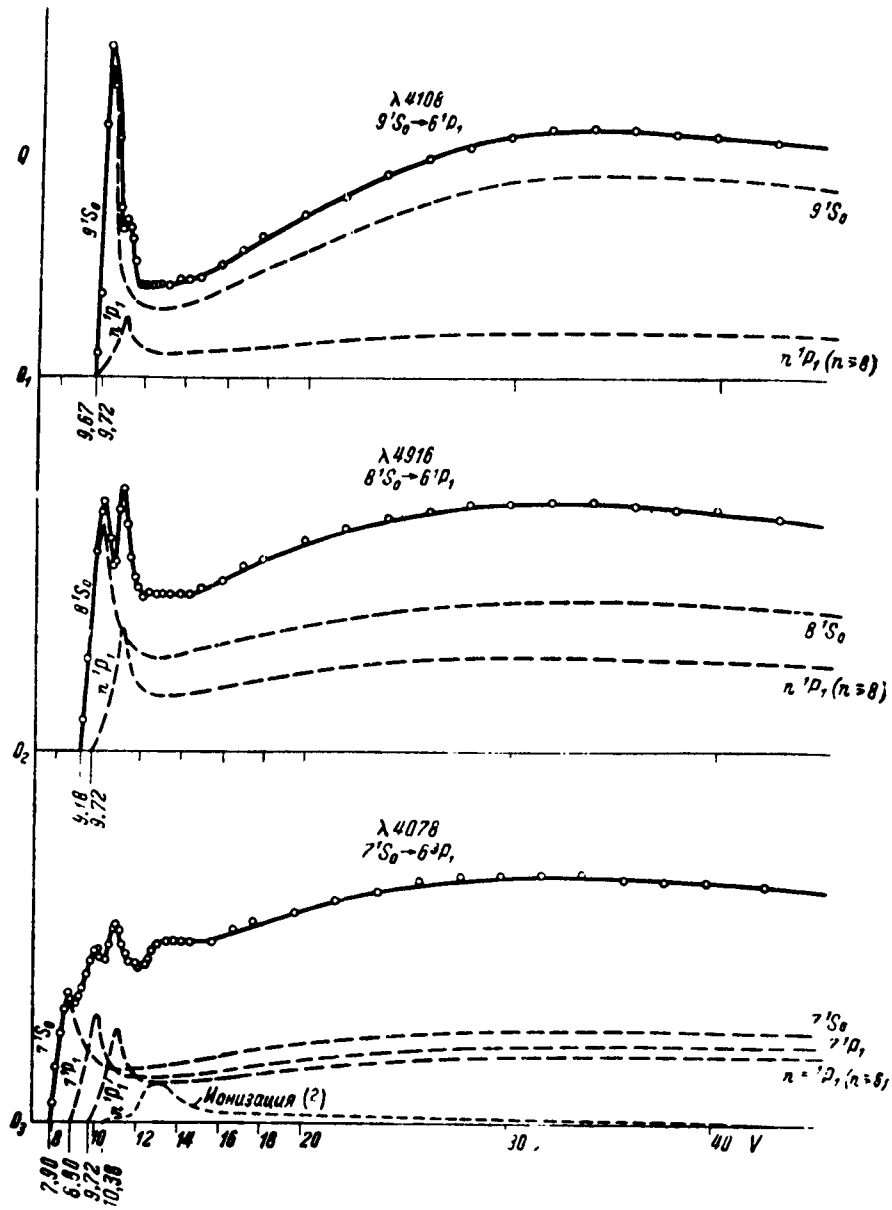


Fig. 18. Layout of the excitation functions of lines λλ 4078, 4916 and 4108 on the excitation function of the separate energy levels.

of line λ 4078 is caused by the excitation of the $7^1S_0$ - level through the cascade transfers from the $7^1P_1$ level which has an excitation potential of 8.8 volts. It is clear that from level $7^1P_1$ transfers can only take place at the $6^1P_0$ and $7^1S_0$ levels, of which the latter is the primary level of line λ 4078. The maxima when V = 11.1 ev for all three lines refer to the excitation of the unsolved group of levels $n^1P_1$ when $n \geqq 8$. Thus, the shape of the curves for these three lines completely correspond to each other. The diffused maximum on the curve for line λ 4078 close to 13 ev, and the plane maxima on the curves of all three lines when there are large energies of the exciting electrons ( V = 30-35 volts ) are still unexplainable. The first of them, perhaps refers to the process of recombination of Hg ions. The origin of the second is unknown; but in all probability, they are inherent to the single excitation functions of the single levels of $n^1S_0$.

Here, it is proper to examine the problem which we have indicated because the excitation functions of the single lines λλ 5791 and 4347 do not show a thin structure. Cascade transfers from the $n^1F_3$ and high $n^1P_1$ levels are possible to the primary levels of these lines $6^1D_2$ and $7^1D_2$, but they are all situated very close to each other. Therefore under operating conditions with that degree of the monokinetic state of the beam, which we obtained, the thin structure consisting of maxima close to each other, could not be solved.

The given arrangements of the optical excitation functions in the excitation function of the separate levels cannot be considered completely identical, but the role of the cascade transfers is doubtless and the revealed nature of the excitation function of the separate levels cannot significantly differ from the actual one near the excitation potential. Divergences are possible when we have potentials which are noticeably larger than the excitation potential.

Therefore, proceeding from the given results, we can compile a table which indicates the position of the maxima of the excitation of the separate levels of an atom of mercury (see Table 2). In all probability, the error in

TABLE 2

| | Triplets | | | | |
|---|---|---|---|---|---|
| | $7^3S_1$ | $7^3P_{012}$ | $8^3P_{012}$ | $9^3P_j$ | $10^3P_j$ and others |
| $V_{crit}$ (critical potential) | 7,7 | 8,6<br>8,6<br>8,8 | 9,4<br>9,4<br>9,5 | 9,8 | 10. 0 and more |
| $V_{max}$ . . | 8,2 | 8,9 | 9,6 | 10,4 | 11,0—11,3 |
| | singlets | | | | |
| | $7^1S_0$ | $8^1S_0$ | $9^1S_0$ | $7^1P_1$ | $8^1P_1$ and others |
| $V_{crit}$ (critical potential) | 7,9 | 9,2 | 9,7 | 8,8 | 9. 7 and more |
| $V_{max}$ . . | 8,7 | 10,1 | 10,4 | 10,0 | 11,0—11,2 |

determining the maxima does not exceed 0. 20-0. 25 volt and is mainly determined by the degree of the monokinetic state of the exciting electrons.

From Table 2 we see that the maxima are peaked for the triplet levels and are very close to the excitation potential (0. 5-0. 2 volts and more); for the single levels, the maxima also have a peaked nature and are also situated close to the excitation potentials, but somewhat further from them than at the triplets (0. 8-1. 2 volts and more).

The results of our work point to the inaccuracy of Schaffernicht's assertion and of other authors about the insignificant role of cascade transfers and about the coincidence of the excitation function of a line with the excitation function of its primary level. Another erroneous assumption of Schaffernicht is that the first maximum in the excitation functions of the lines of the series $6^1P_1$--$n^1S_0$ is caused somehow not by the direct excitation of the upper level, but by the intercombined transfers from the triplet levels; the direct excitation by electrons of the $n^1S_0$ levels (according to Schaffernicht) is revealed in the formation of the horizontal maximum when V = 30-35 volts in the excitation functions of these lines.

It follows from the given material that the excitation functions which have been applied until recently were obtained as a result of the fusion of the curves which refer to the excitation of the separate energy levels. The true excitation functions of the energy levels (of triplets and singlets) have a peaked maximum near the excitation potential.

In the light of the results which we have obtained, we must refute the generally accepted statement that the excitation functions of the single levels, unlike the triplet levels, do not have a peaked maximum near the excitation potential.

In conclusion, I thank Professor S. E. Frish of the Academy of Sciences of the USSR for the theme which he proposed, and for his constant attention and help in this work. I also want to thank Professor S. F. Rodionov and my old colleague A. L. Osherovich for his many valuable recommendations and directions which relate to the usage of the photoelectric photometer.

## LITERATURE

1. Hanle, W. Zeitschrift fur Physik, No. 56: 94, 1929.

2. Ptytsin, S. V. "Fizicheskie iavleniia v oksidnom katode" (Physical phenomena in an oxide cathode), 1929.

3. Osherovich, A. L., E. N. Pavlova, S. F. Rodionov, and L. A. Fishkova. Zhurnal Eksperimental'noi i Teoreticheskoi Fiziki, 19: 184, 1949.

4. Schaffernicht, F. Zeitschrift fur Physik, No. 62: 106, 1930.

5. Frish, S. E. and I. P. Zapesochnyi. Akademiia Nauk, Doklady, 55(5): 971, 1954.

The article was edited on 5 May 1954.